# Atomic population inversion and enhancement of resonance fluorescence in a cavity

Tran Quang and Helen Freedhoff
*Deparment of Physics, York University, 4700 Keele Street, Toronto, Ontario, Canada M3J 1P3*
(Received 14 July 1992)

We investigate properties of a two-level atom coupled to a single cavity mode, and driven by a strong, in general off-resonance, external field. The cavity field is tuned to resonance with a Mollow sideband. We show that the steady-state atomic population may be highly (nearly totally) inverted, a phenomenon forbidden in semiclassical theory, and that a strong enhancement of the resonance fluorescence results. This system is suggested as an alternative approach to create the atomic inversion necessary for laser or maser generation without using additional atomic levels. We also investigate properties of the cavity field, derive an analytical expression for the photon number distribution in the good cavity or strong-coupling limit, and discuss the conditions under which this system acts as a single-atom dressed-state laser.

PACS number(s): 42.50.Hz, 32.80.−t, 42.50.Dv

## I. INTRODUCTION

The properties of a system of atoms interacting with a cavity field have been the subject of intense investigation in recent years in the context of cavity quantum electrodynamics [1]. Many interesting quantum effects have been observed; among these are the enhancement and suppression of spontaneous emission [2–5], vacuum Rabi splitting [6–8], micromaser action [9,10], and the collapse-revivals of the atomic inversion [11].

The system consisting of a single atom coupled strongly to a single quantized cavity mode, and driven by a coherent external field, has been theoretically investigated extensively, including the effects of cavity damping and spontaneous emission. Dynamical suppression of spontaneous emission [12], suppression of fluorescence in a lossless cavity [13], the steady-state spectrum of resonance fluorescence in a cavity [14–16], collapse and revival phenomena in the optical domain [17], single-atom optical bistability [18], photon antibunching and squeezing [19], and the one-atom laser [20] have all been discussed. Very recently, very-high-$Q$ cavities have been constructed for optical frequencies [6,7,21,22], allowing the testing of this model; the vacuum Rabi splitting of a single atom in a cavity has been observed [7].

In this paper, we investigate properties of a two-level atom coupled to a single cavity mode, and driven by a strong external field. Unlike previous works [12–16], we consider an off-resonance external field, with the cavity tuned to resonance with a Mollow sideband. First, it is shown that the steady-state atomic population may be strongly (near totally) inverted, a phenomenon forbidden in semiclassical theory. This result is in sharp contrast to the case of exact resonance [15], where only a very small population inversion has been reported. This scheme is suggested as a quantum approach to create the inversion necessary for laser or maser generation without the use of additional atomic levels. Second, a strong enhancement of the atomic resonance fluorescence is predicted. Finally, we investigate the properties of the cavity field, derive an analytical expression for the photon-number distribution in the strong-coupling limit, and discuss conditions under which this system acts as a single-atom dressed-state laser.

## II. MASTER EQUATION

We consider a two-level atom, with excited state $|2\rangle$, ground state $|1\rangle$, and transition frequency $\omega_a$. The atom is coupled to a cavity mode with coupling constant $g$, driven by a coherent external field at a frequency $\omega_L$ with resonant Rabi frequency $\varepsilon$, and damped at the rate $\gamma$ by spontaneous emission to modes other than the privileged cavity mode. For an optical cavity in which the field mode subtends a small solid angle, $\gamma$ is approximately equal to the Einstein $A$ coefficient. For simplicity, we treat the driving external field classically [12–16]. In the interaction picture the master equation for the system of atom-plus-cavity field has the form [13–16]

$$\frac{\partial}{\partial t}\rho=-i[H,\rho]+\tfrac{1}{2}kL_c\rho+\tfrac{1}{2}\gamma L_a\rho\ , \tag{1}$$

where

$$H=\Delta_c a^\dagger a+\tfrac{1}{2}\Delta_a(\sigma_{22}-\sigma_{11})+g(\sigma_{12}a^\dagger+\sigma_{21}a) +\varepsilon(\sigma_{21}+\sigma_{12})\ , \tag{2}$$

$$L_c\rho=2a\rho a^\dagger-a^\dagger a\rho-\rho a^\dagger a\ , \tag{3}$$

$$L_a\rho=2\sigma_{12}\rho\sigma_{21}-\sigma_{21}\sigma_{12}\rho-\rho\sigma_{21}\sigma_{12}\ . \tag{4}$$

Here $L_c$ and $L_a$ are operators, representing the damping of the field via cavity decay and of the atom via spontaneous emission; $k$ is the cavity decay rate; $a$ and $a^\dagger$ are the cavity-mode (boson) annihilation and creation operators; $\sigma_{ij}$ are the atomic operators $\sigma_{ij}=|i\rangle\langle j|$ $(i,j=1,2)$; $\Delta_a=\omega_a-\omega_L$, $\Delta_c=\omega_c-\omega_L$ are the detuning of the atomic resonance frequency $\omega_a$ and of the cavity-mode frequency $\omega_c$ from the driving field frequency $\omega_L$. Equation (1) is the master equation describing resonance fluorescence of the atom in the cavity and has been integrated numerically for the case of exact resonance $\Delta_a=\Delta_c=0$ in

 

Refs. [15,16]. We focus here on the case with $\Delta_a$ and $\Delta_c$ not necessarily zero.

Equation (1) is written in the basis of the atomic Hilbert space $|i\rangle$, $i=1,2$. We introduce instead the dressed states [23,24]

$$|\tilde{1}\rangle=\cos\phi|1\rangle-\sin\phi|2\rangle\ , \tag{5}$$

$$|\tilde{2}\rangle=\sin\phi|1\rangle+\cos\phi|2\rangle\ , \tag{6}$$

where

$$\cos^2\phi=\tfrac{1}{2}+\frac{\Delta_a}{4\Omega}\ , \tag{7}$$

$\Omega=\frac{1}{2}(\Delta_a^2+4\varepsilon^2)^{1/2}$ is the Rabi frequency in the detuned field; and the "rotation" angle $\phi$ belongs to the interval $[0,(\pi/2)]$. In the basis $|\tilde{i}\rangle$, the operators $\sigma_{ij}$ are replaced by dressed-state operators $R_{ij}=|\tilde{i}\rangle\langle\tilde{j}|$

$$\sigma_{12}=\tfrac{1}{2}\sin(2\phi)R_3-\sin^2\phi R_{21}+\cos^2\phi R_{12}\ , \tag{8}$$

$$\sigma_{21}=\tfrac{1}{2}\sin(2\phi)R_3-\sin^2\phi R_{12}+\cos^2\phi R_{21}\ , \tag{9}$$

$$\sigma_{22}-\sigma_{11}=\cos(2\phi)R_3-\sin(2\phi)(R_{12}+R_{21})\ , \tag{10}$$

$$R_3=R_{22}-R_{11}\ . \tag{11}$$

The master equation is then rewritten in the form

$$\frac{\partial}{\partial t}\rho=-i[\tilde{H}_0+\tilde{H}_{\rm int},\rho]+\tfrac{1}{2}kL_c\rho+\tfrac{1}{2}\gamma\tilde{L}_a\rho\ , \tag{12}$$

where

$$\tilde{H}_0=\Omega R_3+\Delta_c a^\dagger a\ , \tag{13}$$

$$\tilde{H}_{\rm int}=ga^\dagger[\tfrac{1}{2}\sin(2\phi)R_3-\sin^2\phi R_{21}+\cos^2\phi R_{12}]+ga[\tfrac{1}{2}\sin(2\phi)R_3-\sin^2\phi R_{12}+\cos^2\phi R_{21}]\ , \tag{14}$$

and

$$\begin{aligned}\tilde{L}_a\rho=&2[\tfrac{1}{2}\sin(2\phi)R_3-\sin^2\phi R_{21}+\cos^2\phi R_{12}]\rho[\tfrac{1}{2}\sin(2\phi)R_3-\sin^2\phi R_{12}+\cos^2\phi R_{21}]\\&-[\tfrac{1}{2}\sin(2\phi)R_3-\sin^2\phi R_{12}+\cos^2\phi R_{21}][\tfrac{1}{2}\sin(2\phi)R_3-\sin^2\phi R_{21}+\cos^2\phi R_{12}]\rho\\&-\rho[\tfrac{1}{2}\sin(2\phi)R_3-\sin^2\phi R_{12}+\cos^2\phi R_{21}][\tfrac{1}{2}\sin(2\phi)R_3-\sin^2\phi R_{21}+\cos^2\phi R_{12}]\ .\end{aligned} \tag{15}$$

As is well known [24–28], fluorescence of the atom occurs at the laser frequency $\omega_L$ and at the two sideband frequencies $\omega_L\pm2\Omega$.

We now focus on the case of $\Delta_c=2\Omega$, i.e., the cavity field is tuned to exact resonance with the high-frequency sideband (however, we note that the tuning $\Delta_c=-2\Omega$ will produce the same results with $\Delta_a\Longrightarrow-\Delta_a$). We make the unitary transformation

$$\tilde{\rho}=e^{i\tilde{H}_0t}\rho e^{-i\tilde{H}_0t}\ , \tag{16}$$

and ignore rapidly oscillating terms [29,30]. The master Eq. (1) in the dressed state basis reduces to

$$\begin{aligned}\frac{\partial}{\partial t}\tilde{\rho}=&-ig_1[R_{21}a+a^\dagger R_{12},\tilde{\rho}]+\tfrac{1}{2}L_c\tilde{\rho}+\frac{\gamma}{8}\sin^2(2\phi)(2R_3\tilde{\rho}R_3-\tilde{\rho}R_3^2-R_3^2\tilde{\rho})\\&+\frac{\gamma}{2}\cos^4\phi(2R_{12}\tilde{\rho}R_{21}-\tilde{\rho}R_{21}R_{12}-R_{21}R_{12}\tilde{\rho})+\frac{\gamma}{2}\sin^4\phi(2R_{21}\tilde{\rho}R_{12}-\tilde{\rho}R_{12}R_{21}-R_{12}R_{21}\tilde{\rho})\ ,\end{aligned} \tag{17}$$

where

$$g_1=g\cos^2\phi \tag{18}$$

is the "effective" coupling constant. The errors of this "secular approximation" are of order $\gamma/\Omega$, $g_1E_c/\Omega$, where $E_c$ is the amplitude of the cavity field. The approximation is therefore valid when the driving field is strong or the detuning $\Delta_a$ large so that [29,30]

$$\Omega\gg\gamma,g_1E_c\ . \tag{19}$$

In the ideal case of the lossless cavity ($k=0$) and exact resonance ($\Delta_a=\Delta_c=0$), the steady-state cavity field has an amplitude equal to that of the external field [13]. Clearly in this case the secular approximation is not valid. However, as we will see in Sec. V, in realistic cases, the intensity of the cavity field can be small and the condition (19) easily satisfied.

Equation (17) describes the interaction of the dressed atom with the cavity field and vacuum. The last term of Eq. (17), which is proportional to $(\gamma/2)\sin^4\phi$, corresponds to spontaneous emission from the lower dressed state $|\tilde{1}\rangle$ of one manifold to the upper dressed state $|\tilde{2}\rangle$ of the manifold below; hence it plays the role of "pumping" the atom from $|\tilde{1}\rangle$ to $|\tilde{2}\rangle$.

## III. STEADY-STATE SOLUTION

In this section we calculate the steady-state solution of Eq. (17). We introduce density-matrix elements with respect to the two atomic dressed states, denoting $\langle\tilde{2}|\tilde{\rho}|\tilde{1}\rangle$ by $\tilde{\rho}_{21}$, etc. The equations of motion then become

$$\begin{aligned}\frac{\partial}{\partial t}\tilde{\rho}_{11}=&ig_1(\tilde{\rho}_{12}a-a^\dagger\tilde{\rho}_{21})+\gamma\cos^4\phi\tilde{\rho}_{22}\\&-\gamma\sin^4\phi\tilde{\rho}_{11}+\tfrac{1}{2}kL_c\tilde{\rho}_{11}\ ,\end{aligned} \tag{20}$$

$$\frac{\partial}{\partial t}\tilde{\rho}_{22}=ig_1(\tilde{\rho}_{21}a^\dagger-a\tilde{\rho}_{12})-\gamma\cos^4\phi\tilde{\rho}_{22}+\gamma\sin^4\phi\tilde{\rho}_{11}+\tfrac{1}{2}kL_c\rho_{22}\ , \tag{21}$$

$$\frac{\partial}{\partial t}\tilde{\rho}_{12}=ig_1(\tilde{\rho}_{11}a^\dagger-a^\dagger\tilde{\rho}_{22})-\frac{\gamma}{2}[1+\tfrac{1}{2}\sin^2(2\phi)]\tilde{\rho}_{12}+\tfrac{1}{2}kL_c\tilde{\rho}_{12}\ , \tag{22}$$

$$\frac{\partial}{\partial t}\tilde{\rho}_{21}=ig_1(\tilde{\rho}_{22}a-a\tilde{\rho}_{11})-\frac{\gamma}{2}[1+\tfrac{1}{2}\sin^2(2\phi)]\tilde{\rho}_{21}+\tfrac{1}{2}kL_c\tilde{\rho}_{21}\ , \tag{23}$$

We note that the atomic matrix elements $\tilde{\rho}_{ij}$ $(i,j=1,2)$ are still operators with respect to the cavity field mode.

In the case of free-space resonance fluorescence, the steady-state density-matrix elements $\tilde{\rho}_{ij}$, which become $c$ numbers, can be found from Eqs. (20)–(23) to be

$$\tilde{\rho}_{11}^{(\mathrm{sp})}=\frac{\cos^4\phi}{\cos^4\phi+\sin^4\phi}\ , \tag{24}$$

$$\tilde{\rho}_{22}^{(\mathrm{sp})}=\frac{\sin^4\phi}{\cos^4\phi+\sin^4\phi}\ , \tag{25}$$

$$\tilde{\rho}_{12}^{(\mathrm{sp})}=\tilde{\rho}_{21}^{(\mathrm{sp})}=0\ . \tag{26}$$

Using the steady-state solution (24)–(26) one can investigate properties of the atom and fluorescence field, and in particular derive the well-known Mollow triple fluorescence spectrum [24–28].

In the case of resonance fluorescence in the cavity, instead of the four operators $\tilde{\rho}_{ij}$ $(i,j=1,2)$ we use the following Hermitian combinations [17]:

$$\rho^{(1)}=\tilde{\rho}_{22}+\tilde{\rho}_{11}\ , \tag{27}$$

$$\rho^{(2)}=\tilde{\rho}_{22}-\tilde{\rho}_{11}\ , \tag{28}$$

$$\rho^{(3)}=\frac{i}{2}(a\tilde{\rho}_{12}-\tilde{\rho}_{21}a^\dagger)\ , \tag{29}$$

$$\rho^{(4)}=\frac{i}{2}(\tilde{\rho}_{12}a-a^\dagger\tilde{\rho}_{21})\ . \tag{30}$$

We note that

$$\rho^{(1)}=\mathrm{Tr}_A(\rho)=\tilde{\rho}_{22}+\tilde{\rho}_{11} \tag{31}$$

is the reduced density operator of the cavity field. From Eqs. (20)–(23) we obtain equations of motion for $\rho^{(i)}$ in the form

$$\dot{\rho}^{(1)}=\tfrac{1}{2}kL_c\rho^{(1)}-2g_1\rho^{(3)}+2g_1\rho^{(4)}\ , \tag{32}$$

$$\dot{\rho}^{(2)}=-\gamma\cos(2\phi)\rho^{(1)}-\gamma(\cos^4\phi+\sin^4\phi)\rho^{(2)}+\tfrac{1}{2}kL_c\rho^{(2)}-2g_1\rho^{(3)}-2g_1\rho^{(4)}\ , \tag{33}$$

$$\dot{\rho}^{(3)}=\frac{g_1}{4}(\rho^{(1)}aa^\dagger+aa^\dagger\rho^{(1)}-2a\rho^{(1)}a^\dagger)+\frac{g_1}{4}(\rho^{(2)}aa^\dagger+aa^\dagger\rho^{(2)}+2a\rho^{(2)}a^\dagger)-\frac{k}{2}\rho^{(3)}-\frac{\gamma}{2}[1+\tfrac{1}{2}\sin^2(2\phi)]\rho^{(3)}+\tfrac{1}{2}kL_c\rho^{(3)}\ , \tag{34}$$

$$\dot{\rho}^{(4)}=\frac{g_1}{4}(2a^\dagger\rho^{(1)}a-a^\dagger a\rho^{(1)}-\rho^{(1)}a^\dagger a)+\frac{g_1}{4}(2a^\dagger\rho^{(2)}a+a^\dagger a\rho^{(2)}+\rho^{(2)}a^\dagger a)-k\rho^{(3)}+\frac{k}{2}\rho^{(4)}-\frac{\gamma}{2}[1+\tfrac{1}{2}\sin^2(2\phi)]\rho^{(4)}+\tfrac{1}{2}kL_c\rho^{(4)}\ . \tag{35}$$

In contrast to Eqs. (20)–(23), Eqs. (32)–(35) contain only bilinear combinations of photon operators in the form $\rho^{(i)}a^\dagger a, a\rho^{(i)}a^\dagger, \ldots$ . This has the effect of decoupling the equations in the photon-number representation for the diagonal elements $\rho_{n,n}^{(i)}$ and the off-diagonal elements $\rho_{n,n+m}^{(i)}$. The equations of motion for the diagonal matrix elements $P_n^{(i)}\equiv\rho_{n,n}^{(i)}$ $(i=1,\ldots,4;n=0,1,2,\ldots)$ are derived from Eqs. (32)–(35) in the form

$$\dot{P}_n^{(1)}=k(n+1)P_{n+1}^{(1)}-knP_n^{(1)}-2g_1P_{n,n}^{(3)}+2g_1P_n^{(4)}\ , \tag{36}$$

$$\dot{P}_n^{(2)}=-\gamma\cos(2\phi)P_n^{(1)}-\gamma(\cos^4\phi+\sin^4\phi)P_n^{(2)}+k(n+1)P_{n+1}^{(2)}-knP_n^{(2)}-2g_1P_n^{(3)}-2g_1P_n^{(4)}\ , \tag{37}$$

$$\dot{P}_n^{(3)}=\frac{g_1}{2}(n+1)(P_n^{(1)}-P_{n+1}^{(1)}+P_n^{(2)}+P_{n+1}^{(2)})-\tfrac{1}{2}kP_n^{(3)}-\frac{\gamma}{2}[1+\tfrac{1}{2}\sin^2(2\phi)]P_n^{(3)}+k(n+1)P_{n+1}^{(3)}-knP_n^{(3)}\ , \tag{38}$$

$$\dot{P}_n^{(4)}=\frac{g_1}{2}n(P_{n-1}^{(1)}-P_n^{(1)}+P_{n-1}^{(2)}+P_n^{(2)})-kP_n^{(3)}+\tfrac{1}{2}kP_n^{(4)}-\frac{\gamma}{2}[1+\tfrac{1}{2}\sin^2(2\phi)]P_n^{(4)}+k(n+1)P_{n+1}^{(4)}-knP_n^{(4)}\ . \tag{39}$$

We now derive the steady-state solution of Eqs. (36)–(39), setting $\dot{P}_n^{(i)}=0$ $(i=1,\ldots,4)$. Comparing Eqs. (36), (38), and (39), we find that

$$P_n^{(3)}=P_{n+1}^{(4)}=\frac{k}{2g_1}(n+1)P_{n+1}^{(1)}\ . \tag{40}$$

Next, we obtain for the steady state $P_n^{(2)}$ the expression

$$P_n^{(2)}=-\frac{k^2}{g_1^2}\frac{k(n+1)(n+2)}{k(2n+1)+\gamma(\cos^4\phi+\sin^4\phi)}P_{n+2}^{(1)}+\frac{k^2(n+1)}{2g_1^2}\frac{2k(n+\frac{1}{2})+\gamma[1+\frac{1}{2}\sin^2(2\phi)]}{k(2n+1)+\gamma(\cos^4\phi+\sin^4\phi)}P_{n+1}^{(1)}-\frac{k(2n+1)+\gamma\cos(2\phi)}{k(2n+1)+\gamma(\cos^4\phi+\sin^4\phi)}P_n^{(1)}\ , \tag{41}$$

and for $P_n^{(1)}$ the recurrence relation

$$\frac{k^2}{g_1^2}\frac{k(n+2)(n+3)}{k(2n+3)+\gamma(\cos^4\phi+\sin^4\phi)}P_{n+3}^{(1)}$$
$$-\frac{k^2}{g_1^2}(n+2)\left[\frac{kn+\gamma(\cos^4\phi+\sin^4\phi)}{k(2n+1)+\gamma(\cos^4\phi+\sin^4\phi)}+\frac{k(n+\frac{3}{2})+\frac{\gamma}{2}[1+\frac{1}{2}\sin^2(2\phi)]}{k(2n+3)+\gamma(\cos^4\phi+\sin^4\phi)}\right]P_{n+2}^{(1)}$$
$$+\frac{k^2}{g_1^2}\left[n+\tfrac{1}{2}+\frac{\gamma}{2k}[1+\tfrac{1}{2}\sin^2(2\phi)]-(n+1)\frac{k(n+\frac{1}{2})+\frac{\gamma}{2}[1+\frac{1}{2}\sin^2(2\phi)]}{k(2n+1)+\gamma(\cos^4\phi+\sin^4\phi)}\right]P_{n+1}^{(1)}$$
$$+\frac{2k(2n+3)+2\gamma\cos^4\phi}{k(2n+3)+\gamma(\cos^4\phi+\sin^4\phi)}P_{n+1}^{(1)}-\frac{2\gamma\sin^4\phi}{k(2n+1)+\gamma(\cos^4\phi+\sin^4\phi)}P_n^{(1)}=0\ . \quad (42)$$

We have calculated $P_n^{(1)}$ from Eq. (42) by using a truncated basis of number states. The validity of the truncation was ensured by requiring that $P_n^{(1)}$ not change as the number of truncated states was increased.

Equations for the off-diagonal density-matrix elements $\rho_{n,n+m}^{(i)}$ ($i=1,\ldots,4; n=0,1,2,\ldots,; m=1,2,\ldots$) can be derived analogously from Eqs. (32)–(35). Using these equations we can easily show that all steady-state off-diagonal elements $\rho_{n,n+m}^{(i)}$ equal to zero.

## IV. ATOMIC POPULATION INVERSION AND ENHANCEMENT OF RESONANCE FLUORESCENCE

In this section we investigate the influence of the cavity on the steady-state atomic population and on the fluorescence intensity. In free space, the population inversion between the dressed states $|\tilde{2}\rangle$ and $|\tilde{1}\rangle$ is calculated using Eqs. (24) and (25):

$$\langle R_3\rangle_{\rm sp}=\tilde{\rho}_{22}^{(\rm sp)}-\tilde{\rho}_{11}^{(\rm sp)}=-\frac{\cos(2\phi)}{\cos^4\phi+\sin^4\phi}\ . \quad (43)$$

Using Eq. (10) and noting that the steady-state off-diagonal density-matrix elements $\tilde{\rho}_{12}^{(\rm sp)}=\tilde{\rho}_{21}^{(\rm sp)}=0$. We calculate the population inversion between the bare atom excited state $|2\rangle$ and ground state $|1\rangle$ to be

$$\Delta P_{\rm sp}\cong\langle\sigma_{22}\rangle-\langle\sigma_{11}\rangle=\cos(2\phi)\langle R_3\rangle_{\rm sp}$$
$$=-\frac{\cos^2(2\phi)}{\cos^4\phi+\sin^4\phi}\ . \quad (44)$$

Clearly $\Delta P_{\rm sp}\le 0$, i.e., interaction with the classical field does not lead to a population inversion in the two-level atomic system. Additional atomic levels must be used in order to create the population inversion necessary for laser or maser generation [31].

In the cavity, the steady-state atomic population inversion in the dressed-state basis takes the form

$$\langle R_3\rangle={\rm Tr}_{\rm field}(\rho^{(2)})=\sum_{n=0}^{\infty}P_n^{(2)}\ , \quad (45)$$

where $P_n^{(2)}$ is given in Eq. (41) in terms of the photon-number distribution $P_n^{(1)}$. Because the steady-state off-diagonal density-matrix elements $\rho_{n,n+m}^{(i)}$ equal zero, we can easily derive

$$(\tilde{\rho}_{12})_{n,n}=(\tilde{\rho}_{21})_{n,n}=0\ , \quad (46)$$

analogous to Eq. (26) for the free-space case. With the help of Eqs. (10) and (46) we obtain for the steady-state atomic population inversion (between the bare states) the expression

$$\Delta P=\cos(2\phi)\langle R_3\rangle=\cos(2\phi)\sum_{n=0}^{\infty}P_n^{(2)}\ . \quad (47)$$

In Fig. 1 we plot the atomic population inversion $\Delta P$, Eq. (47) as a function of the scaled detuning $\delta=\Delta_a/2\varepsilon$ for fixed $k/g$ and various values of $k/\gamma$, comparing it with the case of free space, Eq. (44). Clearly for $\gamma>g,k$ (long-short-dashed curve) the influence of the cavity on the atomic behavior is small and the population inversion $\Delta P$ differs only slightly from that of free space (dotted curve). With increasing cavity decay rate $k$, $\Delta P$ increases and even becomes positive in a large region of $\delta<0$ (long-dashed, short-dashed, and solid curves). For $k\gg\gamma$ (Fig. 2) the atomic population is very highly inverted and even reaches a nearly total inversion: for the case of $k/g=0.15$ and $k/\gamma=10^3$ (solid curve in Fig. 2) nearly

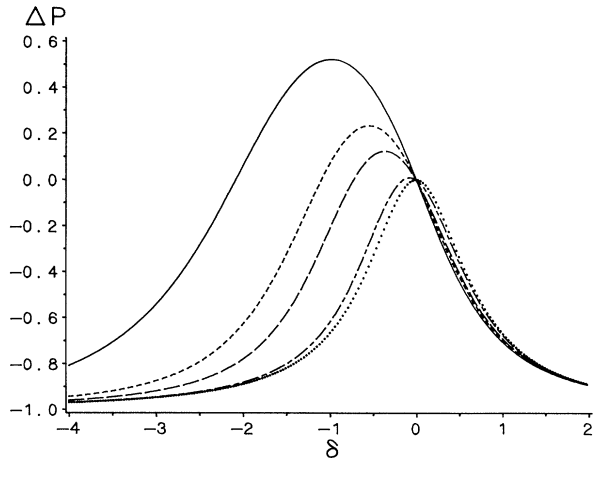


FIG. 1. Atomic population inversion $\Delta P$ as a function of scaled detuning $\delta=\Delta_a/2\varepsilon$ for $k/g=0.3$ and for $k/\gamma=0.2$ (short-long-dashed curve), 1 (long-dashed curve), 2 (short-dashed curve), and 10 (solid curve). The dotted curve corresponds to the case of free space.

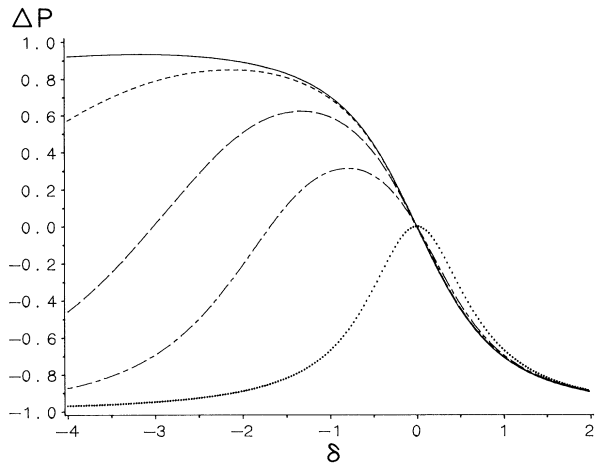


FIG. 2. Atomic population inversion $\Delta P$ as a function of scaled detuning $\delta$ for $k/g=0.15$ and for $k/\gamma=2$ (short-long-dashed curve); 10 (long-dashed curve); $10^2$ (short-dashed curve); and $10^3$ (solid curve). The dotted curve corresponds to the case of free space.

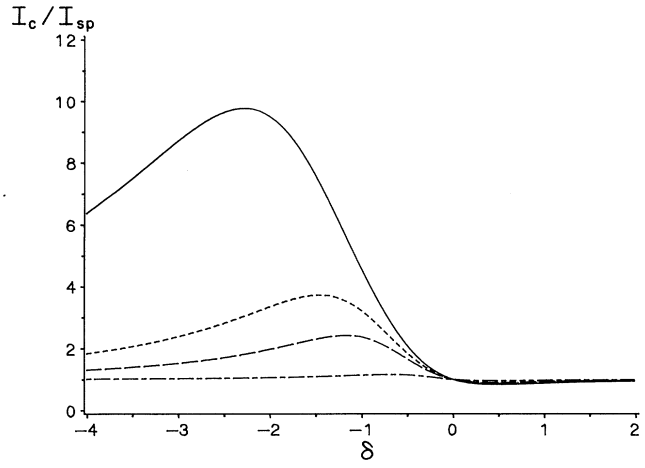


FIG. 3. Ratio between intensities of resonance fluorescence in the cavity and in free space, $I_c/I_{sp}$ as a function of scaled detuning $\delta$ for $k/g=0.3$ and for $k/\gamma=0.2$ (short-long-dashed curve); 1 (long-dashed curve); 2 (short-dashed curve); and 10 (solid curve).

97% of the atomic population is in the excited state $|2\rangle$. As is well known, two-level atomic population inversion is not possible in free space; thus strong steady-state atomic population inversion is a feature of resonance fluorescence in a cavity. These results are in sharp contrast with the case of exact resonance, where only a very small $\Delta P \cong 0.028$ is reported [15].

This effect has a clear physical interpretation: In the steady-state, detailed balance requires that [24]

$$\tilde{\rho}_{22}\Gamma_{\tilde{2}\Longrightarrow\tilde{1}}=\tilde{\rho}_{11}\Gamma_{\tilde{1}\Longrightarrow\tilde{2}} , \tag{48}$$

where $\Gamma_{\tilde{i}\Longrightarrow\tilde{j}}$ is the total transition rate from $|\tilde{i}\rangle$ to $|\tilde{j}\rangle$. The cavity with large $k$, which is tuned to resonance with the dressed-state transition $|\tilde{2}\rangle \Longrightarrow |\tilde{1}\rangle$, strongly enhances the transition rate $\Gamma_{\tilde{2}\Longrightarrow\tilde{1}}$ from $|\tilde{2}\rangle$ to $|\tilde{1}\rangle$ compared to that of free space [5,14]; this in turn requires an increase in the population $\tilde{\rho}_{11}$ to maintain detailed balance. The dressed state $|\tilde{1}\rangle$ is a superposition of the bare atomic states $|1\rangle$ and $|2\rangle$ [Eq. (5)]. For $\Delta_a<0$ (i.e., $\cos\phi<\sin\phi$), increasing the population $\tilde{\rho}_{11}$ is equivalent to increasing the population of the excited state $|2\rangle$, and consequently $\Delta P$, of the bare atom.

The total intensity of the atomic fluorescence, radiated out the sides of the cavity, is proportional to the population of the atomic excited state [12–16,23,24]

$$I\sim\gamma\langle\sigma_{22}\rangle=\frac{\gamma}{2}(1+\Delta P) , \tag{49}$$

where $\Delta P$ is given by Eq. (47) for the cavity, and by Eq. (44) for free space. The increasing population in state $|2\rangle$ thus leads to an enhancement of the resonance fluorescence intensity. In Fig. 3 we plot the ratio between fluorescence intensities in the cavity $I_c$ and in free space $I_{sp}$. Clearly the cavity, especially the cavity with large decay rate $k$, strongly enhances the total fluorescence.

It is useful to note that although we consider here only the case of a single-mode cavity, corresponding to experiments performed by Raizen *et al.* [6], Thompson *et al.* [7], and Rempe *et al.* [21,22], an analogous result would also be obtained in the case of a large number of modes having the same frequency [5]. The steady-state inversion of a population of two-level atoms is in itself an interesting quantum effect, forbidden in semiclassical theory. The above-described scheme may also be useful as a method to create the atomic population inversion necessary for laser or maser generation without the use of additional atomic levels.

## V. STATISTICAL PROPERTIES OF THE CAVITY FIELD

In the previous section, we focused on the bad cavity, in which the influence of the cavity on the atomic population and fluorescent intensity is strong. In this section, we investigate the statistical properties of the cavity field and focus mainly on the case of the good cavity. In particular, we derive an analytical expression for the steady-state photon-number distribution in the good cavity or strong-coupling limit.

We calculate the mean photon number

$$\langle n\rangle=\sum_{n=0}^{\infty} nP_n^{(1)} \tag{50}$$

and normalized variance (Mandel $q$ parameter) [32]

$$q=\frac{\langle n^2\rangle-\langle n\rangle^2}{\langle n\rangle}-1 , \tag{51}$$

where

$$\langle n^2\rangle=\sum_{n=0}^{\infty} n^2P_n^{(1)} . \tag{52}$$

The normalized variance $q$ is used to characterize the deviation from Poissonian statistics. A negative (positive) $q$ value indicates sub-Poissonian (super-Poissonian) statis-

tics, while $q=0$ corresponds to a Poissonian distribution. In particular, the case of $q=-1$ corresponds to 100% noise reduction. The photon-number distribution $P_n^{(1)}$ is calculated numerically from Eq. (42) by using a truncated basis of number states.

In Fig. 4 we plot the mean photon number $\langle n \rangle$ of the cavity field as a function of the scaled detuning $\delta=\Delta_a/2\varepsilon$ for $k/g=0.01$ and for various values of $k/\gamma$. Clearly for $\delta>0$, i.e., $\omega_a>\omega_L$, $\langle n \rangle$ is very small, while for $\delta<0$, $\langle n \rangle$ is significantly larger. This difference is emphasized if the cavity decay rate $k$ is much smaller than the spontaneous emission rate $\gamma$ (solid and long-dashed curves), and can be understood as follows. For $\delta<0$, the driving field creates a population inversion between the dressed states $|\tilde{2}\rangle$ and $|\tilde{1}\rangle$ [ see Eq. (43)]. As a result, the process of stimulated emission into the cavity field dominates absorption from that field, in analogy with the amplification that would occur of a probe field at $\omega_L+2\Omega$ [24]. Equation (17) is the same as the master equation of the dressed-state laser [30] for the single active atom case. As discussed in Sec. II, the term in Eq. (17) which is proportional to $(\gamma/2)\sin^4\phi$ has the effect of pumping the atom from the lower dressed state $|\tilde{1}\rangle$ to the upper dressed state $|\tilde{2}\rangle$, while $k$ is the loss rate of the cavity field. As occurs also in laser generation [31], the amplification coefficient of the dressed-state laser is proportional to a product of the pumping rate and the "effective" coupling constant $g_1$. As a result, for constant $k/g$ the mean photon number $\langle n \rangle$ increases as the ratio between the pumping rate $(\gamma/2)\sin^4\phi$ and cavity decay rate $k$ increases, as is shown in Fig. 4; for $\delta \ll 0$, $g_1=g\cos^2\phi$ becomes very small, causing $\langle n \rangle$ to decrease for all $k/\gamma$. The system acts in this case as a one-atom dressed-state laser, in agreement with recent publications on the dressed-state laser [30,33]. For $\delta>0$, on the other hand, no net stimulated emission can occur at the cavity frequency and the mean photon number of the cavity field remains very small.

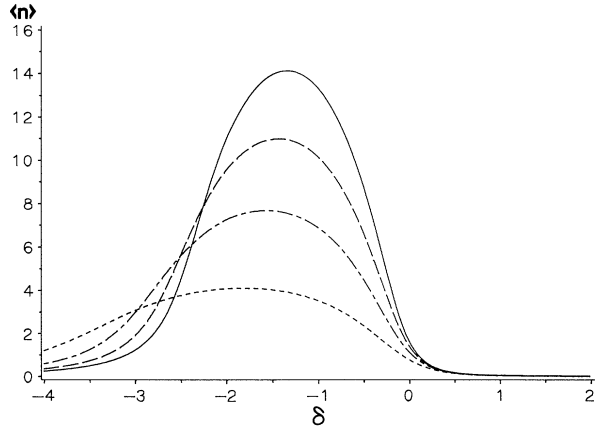


FIG. 4. Mean photon number $\langle n \rangle$ as a function of scaled detuning $\delta$ for $k/g=0.01$ and for $k/\gamma=0.1$ (short-dashed curve), 0.05 (short-long-dashed curve), $\frac{1}{30}$ (long-dashed curve), and 0.025 (solid curve).

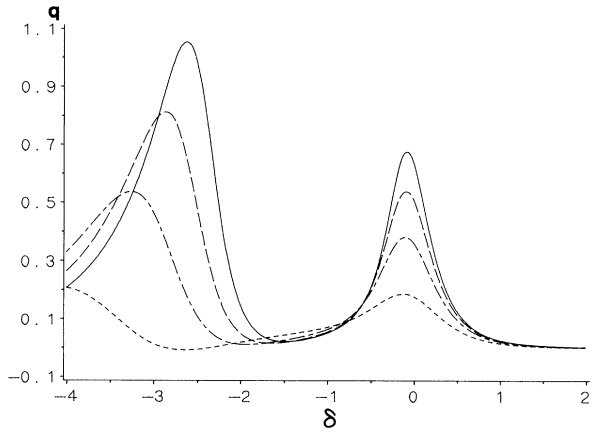


FIG. 5. The Mandel $q$ parameter as a function of $\delta$ for the same parameters as in Fig. 4.

In Fig. 5 we plot the Mandel $q$ parameter as a function of $\delta$ for the same parameters $k/g$, $k/\gamma$ as in Fig. 4. Clearly the normalized variance $q$ is large in the region of $\delta\approx 0$ and $\delta \ll 0$, while for the values of $\delta$ where $\langle n \rangle$ is large $q$ is small and even tends to zero, as it does for coherent states. In Fig. 6 we plot the variance $q$ as a function of $\delta$ for the case of $k=\gamma$ and for various values of $k/g$. Clearly, for a wide range of $\delta$ the photon statistics of the cavity field become sub-Poissonian. However, we note that the mean photon number in the case of $k=\gamma$ is small ($\langle n \rangle \approx 0.5$), and the degree of quantum noise reduction is only about 14%.

For the good cavity or strong-coupling limit

$$\frac{k^2}{g_1^2}\equiv\frac{k^2}{g^2\cos^4\phi}\ll 1\ , \tag{53}$$

all terms of order $k^2/g_1^2$ in Eq. (42) are neglected. Equation (42) then reduces to

$$P_n^{(1)}=\zeta_n P_{n-1}^{(1)}\ , \tag{54}$$

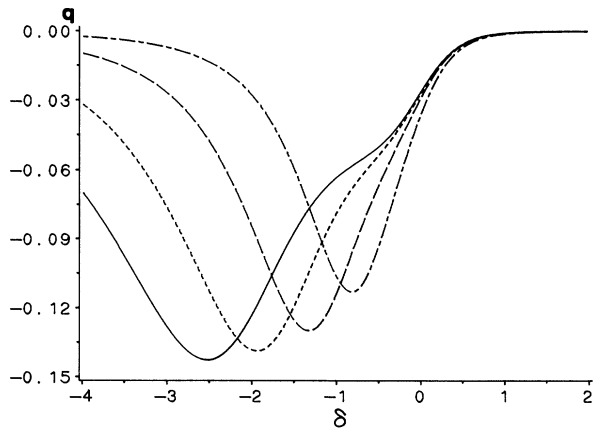


FIG. 6. Mandel $q$ parameter as a function of $\delta$ for $k/\gamma=1$ and for $k/g=0.3$ (short-long-dashed curve), 0.15 (long-dashed curve), 0.008 (short-dashed curve), and 0.05 (solid curve).

where

$$\zeta_n = \left[ \frac{\cos^4\phi + \sin^4\phi + \frac{k}{\gamma}(2n+1)}{\cos^4\phi + \sin^4\phi + \frac{k}{\gamma}(2n-1)} \right] \times \left[ \frac{\sin^4\phi}{\cos^4\phi + \frac{k}{\gamma}(2n+1)} \right] . \quad (55)$$

With Eqs. (54) and (55) we find the steady-state photon-number distribution for the cavity field

$$P_n^{(1)} = P_0^{(1)} \prod_{m=1}^{n} \zeta_m , \quad (56)$$

where $P_0^{(1)}$ is a normalization constant.

The mean photon number $\langle n \rangle$ is plotted in Fig. 7 as a function of the scaled detuning $\delta$. The solid and dashed curves correspond to the numerical evaluation of $P_n^{(1)}$ from Eq. (42) for $k/\gamma = \frac{1}{30}$, and for various values of $k/g$. The dotted curve corresponds to the analytical solution (56) for the same parameter $k/\gamma = \frac{1}{30}$. Clearly, reducing the parameter $k/g$ causes the region of validity of the analytical solution (56) to become wider.

For $k \ll \gamma$, Eq. (55) reduces to

$$\zeta_n = \frac{\sin^4\phi}{\cos^4\phi + \frac{k}{\gamma}(2n+1)} . \quad (57)$$

For $\delta > 0$, $\langle n \rangle$ is small (see Figs. 4 and 7), and Eq. (57) reduces to

$$\zeta_n \cong \frac{\sin^4\phi}{\cos^4\phi} < 1 . \quad (58)$$

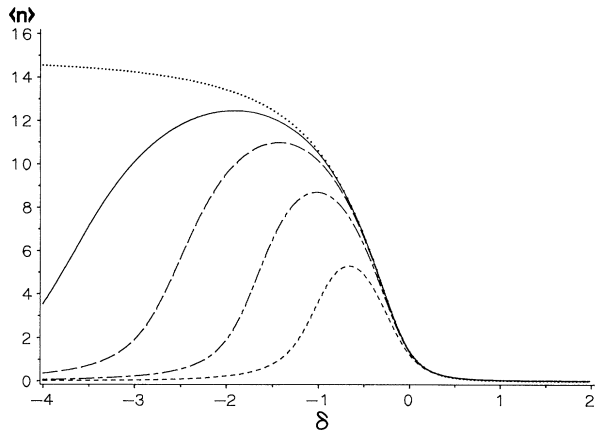


FIG. 7. Mean photon number $\langle n \rangle$ as a function of $\delta$ for $k/\gamma = \frac{1}{30}$ and for $k/g = 0.04$ (short-dashed curve), 0.02 (short-long-dashed curve), 0.01 (long-dashed curve), and 0.005 (solid curve). The dotted curve corresponds to the analytical photon-number distribution (56) for the same parameter $k/\gamma = \frac{1}{30}$.

In this case the photon-number distribution (56) becomes a thermal distribution

$$P_n^{(1)} = \frac{\langle n \rangle^n}{(\langle n \rangle + 1)^{n+1}} , \quad (59)$$

where

$$\langle n \rangle = \frac{\sin^4\phi}{\cos(2\phi)} . \quad (60)$$

For values of $\delta$ such that $\langle n \rangle \gg 1$ (see Figs. 4 and 7), Eq. (57) reduces to

$$\zeta_n \cong \frac{\gamma \sin^4\phi}{2kn} , \quad (61)$$

and the photon-number distribution (56) becomes Poissonian, as in the laser operated far above threshold [31]

$$P_n^{(1)} = e^{-\langle n \rangle} \frac{\langle n \rangle^n}{n!} , \quad (62)$$

where

$$\langle n \rangle = \frac{\gamma \sin^4\phi}{2k} . \quad (63)$$

This result is in agreement with the results shown in Fig. 7, where for values of $\delta$ corresponding to large $\langle n \rangle$, the photon-number variance $q$ tends to zero.

In this paper we studied the case of only a single atom in the cavity. If $N$ atoms are simultaneously present, the collective coupling constant $g\sqrt{N}$ will play an important role [14]. In this case the strong-coupling requirement $g\sqrt{N} \gg k, \gamma$, for $N$ atoms, is less restrictive than that for a single atom, and the experimental requirements to see the effects discussed above can be more easily met [6,7].

## VI. CONCLUSION

In this paper we investigate the atomic and cavity field properties in the problem of resonance fluorescence of an atom in a cavity. Unlike previous publications, we consider the case when the driving field is detuned from the atomic transition frequency, and the cavity is tuned to resonance with a Mollow sideband. We show that in the bad-cavity case the steady-state atomic population is highly inverted, a phenomenon forbidden in semiclassical theory. This system is suggested as a way to create the atomic inversion necessary for laser or maser generation without using additional atomic levels. Under certain conditions, the fluorescent intensity out the sides of the cavity is strongly enhanced above the free-space value. We also investigate the statistical properties of the cavity field, deriving an analytical expression for the photon-number distribution in the strong-coupling limit, and discuss the conditions under which the system acts as a single-atom dressed-state laser.

## ACKNOWLEDGMENT

This research was supported in part by the Natural Sciences and Engineering Research Council of Canada, to whom the authors extended their thanks.

[1] S. Haroche and D. Kleppner, Phys. Today **42**, 24 (1989), and references therein.
[2] E. M. Purcell, Phys. Rev. **69**, 681 (1946).
[3] D. Kleppner, Phys. Rev. Lett. **47**, 232 (1981).
[4] P. Goy, J. M. Raimond, M. Gross, and S. Haroche, Phys. Rev. Lett. **50**, 1903 (1983).
[5] D. J. Heinzen, J. J. Childs, J. E. Thomas, and M. S. Feld, Phys. Rev. Lett. **58**, 1320 (1987).
[6] M. G. Raizen, R. J. Thompson, R. J. Brecha, H. J. Kimble, and H. J. Carmichael, Phys. Rev. Lett. **63**, 240 (1989).
[7] R. J. Thompson, G. Rempe, and H. J. Kimble, Phys. Rev. Lett. **68**, 1132 (1992).
[8] J. J. Sanchez-Mondragon, N. B. Narozhny, and J. H. Eberly, Phys. Rev. Lett. **51**, 550 (1983); G. S. Agarwal, *ibid.* **53**, 1732 (1984).
[9] D. Meschede, H. Walther, and G. Muller, Phys. Rev. Lett. **54**, 551 (1985); M. Brune, J. M. Raimond, P. Goy, L. Davidovich, and S. Haroche, *ibid.* **59**, 1899 (1987).
[10] P. Filipowicz, J. Javanainen, and P. Meystre, Phys. Rev. A **34**, 4547 (1966); L. Lugiato, M. O. Scully, and H. Walther, *ibid.* **36**, 740 (1987); M. O. Scully, H. Walther, G. S. Agarwal, Tran Quang, and W. Schleich, *ibid.* **44**, 5992 (1991).
[11] G. Rempe, H. Walther, and N. Klein, Phys. Rev. Lett. **58**, 353 (1987); E. T. Jaynes and F. W. Cumming, Proc. IEEE **51**, 89 (1963); J. H. Eberly, N. B. Narozhny, and J. J. Sanchez-Mondragon, Phys. Rev. Lett. **23**, 44 (1980); P. Meystre, G. Rempe, and H. Walther, Opt. Lett. **13**, 1078 (1988).
[12] M. Lewenstein, T. W. Mossberg, and R. J. Glauber, Phys. Rev. Lett. **59**, 775 (1987).
[13] P. M. Alsing, D. A. Cardimona, and H. J. Carmichael, Phys. Rev. A **45**, 1793 (1992).
[14] H. J. Carmichael, R. J. Brecha, M. G. Raizen, H. J. Kimble, and P. R. Rice, Phys. Rev. **40**, 5516 (1989).
[15] C. M. Savage, Phys. Rev. Lett. **60**, 1829 (1988); M. Lindberg and C. M. Savage, Phys. Rev. A **38**, 5182 (188).
[16] C. M. Savage, Phys. Rev. Lett. **63**, 1376 (1989); J. Mod. Opt. **37**, 1711 (1990).
[17] Tran Quang, P. L. Knight, and V. Buzek, Phys. Rev. A **44**, 6092 (1991).
[18] C. M. Savage and H. J. Carmichael, IEEE. J. Quantum Electron. **24**, 1495 (1988).
[19] H. J. Carmichael, Phys. Rev. Lett. **55**, 2790 (1985); H. J. Carmichael, R. J. Brecha, and P. R. Rice, Opt. Commun. **82**, 73 (1991); P. R. Rice and H. J. Carmichael, J. Opt. Soc. Am. B **5**, 1661 (1988).
[20] Tran Quang and H. S. Freedhoff, J. Mod. Opt. (to be published).
[21] G. Rempe, R. J. Thompson, R. J. Brecha, W. D. Lee, and H. J. Kimble, Phys. Rev. Lett. **67**, 1727 (1991).
[22] G. Rempe, R. J. Thompson, H. J. Kimble, and R. Lalerari, Opt. Lett. **17**, 363 (1992).
[23] C. Cohen-Tannoudji and S. Reynaud, J. Phys. B **10**, 345 (1977).
[24] C. Cohen-Tannoudji, J. Dupont-Roc, and G. Grynberg, in *Atom-Photon Interaction* (Wiley-Interscience, New York, 1992), Chap. VI.
[25] B. R. Mollow, Phys. Rev. **188**, 1969 (1969).
[26] F. Schuda, C. R. Stroud, and M. Hercher, J. Phys. B **7**, L198 (1979).
[27] W. Hartig, W. Resmassen, R. Schieder, and H. Walther, Z. Phys. A **278**, 205 (1976).
[28] F. Y. Wu, R. E. Grove, and S. Ezekiel, Phys. Rev. Lett. **35**, 1926 (1975).
[29] G. S. Agarwal, L. M. Narducci, D. H. Feng, and R. Gilmore, Phys. Rev. Lett. **42**, 1260 (1978); Tran Quang, M. Kozierowski, and Le Hong Lan, Phys. Rev. A **39**, 644 (1989).
[30] J. Zakrzewski, M. Lewenstein, and T. W. Mossberg, Phys. Rev. A **44**, 7717 (1991).
[31] M. Sargent, M. O. Scully, and W. E. Lamb, *Laser Physics* (Addison-Wesley, Reading, MA, 1974).
[32] L. Mandel, Opt. Lett. **4**, 205 (1979).
[33] M. Lewenstein, Y. Zhu, and T. W. Mossberg, Phys. Rev. Lett. **64**, 3131 (1990).